A&A 650, A1 (2021)
https://doi.org/10.1051/0004-6361/202039354

Astronomy & Astrophysics

Parker Solar Probe: Ushering a new frontier in space exploration

Special issue

Statistical analysis of orientation, shape, and size of solar wind switchbacks

R. Laker[1], T. S. Horbury[1], S. D. Bale[1,2,3], L. Matteini[1], T. Woolley[1], L. D. Woodham[1], S. T. Badman[2,3], M. Pulupa[3], J. C. Kasper[4,5], M. Stevens[4], A. W. Case[4], and K. E. Korreck[4]

[1] Imperial College London, South Kensington Campus, London SW7 2AZ, UK
e-mail: ronan.laker15@imperial.ac.uk
[2] Physics Department, University of California, Berkeley, CA 94720-7300, USA
[3] Space Sciences Laboratory, University of California, Berkeley, CA 94720-7450, USA
[4] Smithsonian Astrophysical Observatory, Cambridge, MA 02138, USA
[5] Climate and Space Sciences and Engineering, University of Michigan, Ann Arbor, MI 48109, USA

Received 7 September 2020 / Accepted 14 October 2020

ABSTRACT

Context. One of the main discoveries from the first two orbits of Parker Solar Probe (PSP) was the presence of magnetic switchbacks, whose deflections dominated the magnetic field measurements. Determining their shape and size could provide evidence of their origin, which is still unclear. Previous work with a single solar wind stream has indicated that these are long, thin structures although the direction of their major axis could not be determined.
Aims. We investigate if this long, thin nature extends to other solar wind streams, while determining the direction along which the switchbacks within a stream were aligned. We try to understand how the size and orientation of the switchbacks, along with the flow velocity and spacecraft trajectory, combine to produce the observed structure durations for past and future orbits.
Methods. The direction at which the spacecraft cuts through each switchback depended on the relative velocity of the plasma to the spacecraft and the alignment direction for that stream. We searched for the alignment direction that produced a combination of a spacecraft cutting direction and switchback duration that was most consistent with long, thin structures. The expected form of a long, thin structure was fitted to the results of the best alignment direction, which determined the width and aspect ratio of the switchbacks for that stream.
Results. We find that switchbacks consistently demonstrate a non-radial alignment in the same sense as the Parker spiral field, but not the background flow direction within each stream. This alignment direction varied between streams. The switchbacks had a mean width of 50 000 km, with an aspect ratio of the order of 10.
Conclusions. We conclude that switchbacks are not aligned along the background flow direction, but instead aligned along the local Parker spiral, perhaps suggesting that they propagate along the magnetic field. Since the observed switchback duration depends on how the spacecraft cuts through the structure, the duration alone cannot be used to determine the size or influence of an individual event. For future PSP orbits, a larger spacecraft transverse component combined with more radially aligned switchbacks will lead to long duration switchbacks becoming less common.

Key words. Sun: heliosphere – solar wind – Sun: magnetic fields

1. Introduction

Parker Solar Probe (PSP) began a new era for heliophysics when it surpassed the Helios probes as the closest spacecraft to measure the solar wind at 35 solar radii from the Sun. Bale et al. (2019) and Kasper et al. (2019) report the dominance of 'switchbacks' in the magnetic field, discrete large angular deflections from the background magnetic field direction lasting from seconds to hours (Dudok de Wit et al. 2020). Being Alfvénic in nature (Matteini et al. 2014), these switchbacks are associated with an increase in plasma velocity and therefore are an important contribution to the overall mass flux of the solar wind.

Switchbacks have previously been observed with data from Helios (Horbury et al. 2018) and Ulysses (Balogh et al. 1999; Neugebauer & Goldstein 2013), but it was the magnitude and prevalence of the switchbacks that made the PSP observations striking. Switchbacks have been shown to be consistent with folds in the magnetic field, rather than reversals in local polarity (Balogh et al. 1999; Mcmanus et al. 2020). Horbury et al. (2020) describe the magnetic field vectors within switchbacks as being arc-polarised rotations on a sphere of constant $|\boldsymbol{B}|$, while also showing that the direction of switchback deflection was broadly consistent on the timescales of hours to days.

The origin of these structures is still unclear, whether they are a product of fluctuations expanding with the solar wind (Squire et al. 2020), or the remnants of transient events originating in the solar corona (Horbury et al. 2020; Sterling & Moore 2020). One such example of a transient coronal event are coronal jets, which have been studied in extreme ultraviolet (EUV) and X-ray observations (Raouafi et al. 2016). Dudok de Wit et al. (2020) demonstrate, with waiting time statistics, that the switchbacks are correlated and exhibit a long term memory, which supports the idea of a coronal origin. A key assumption of the coronal origin theory is that fluctuations can survive out to the distances of PSP. This has been shown to be possible with recent magnetohydrodynamic (MHD) simulations when $|\boldsymbol{B}|$ is constant

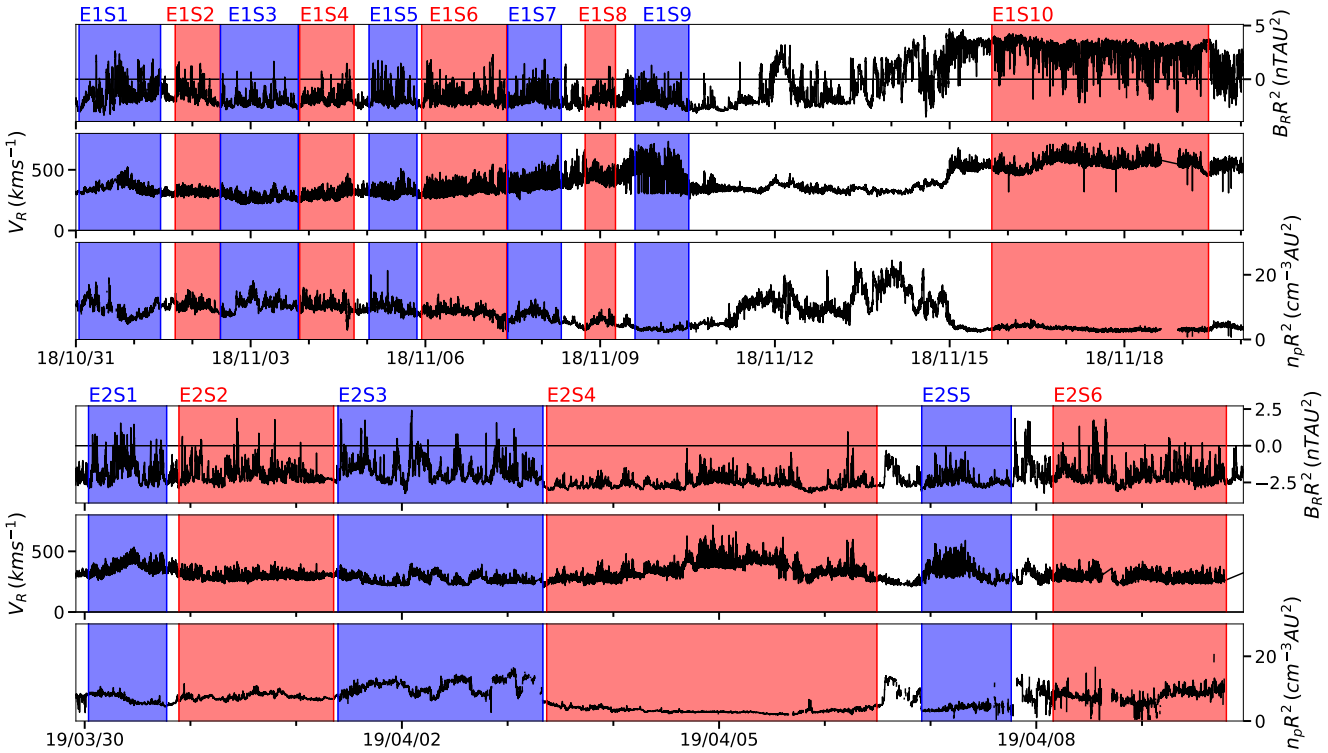

Fig. 1. Summary of solar wind streams for encounters 1 and 2, along with their identification numbers. All streams in encounter 1 (except *E1S*10) are from the same equatorial coronal hole. The period between *E1S*9 and *E1S*10 was ignored, as this is a heliospheric current sheet crossing (Szabo et al. 2020). Encounter 2 streams were picked according to the Rouillard et al. (2020) classification of non and streamer belt solar wind. A more detailed summary of these streams can be found in Table A.1. The *top panels* for both encounters show B_R multiplied by the radial distance to the Sun squared. This is an attempt to remove the first order variation in B_R, normalising the switchback amplitude with distance.

(Tenerani et al. 2020), but it is unclear whether this extends to larger distances, such as the Ulysses observations (Neugebauer & Goldstein 2013). Although switchbacks are the dominant signal in PSP's first encounter, they are not ubiquitous, occurring in 'patches' separated by a 'quiet' radial field (Bale et al. 2019; Horbury et al. 2020). These quiet regions exhibit a wide array of kinetic wave activity that is not seen in the patches (Verniero et al. 2020; Bowen et al. 2020). This combined with differences in magnetic compressibility could indicate that patches of switchbacks are impulsive events overlain on a fundamentally different background plasma (Woodham et al. 2021). This observation may prove to be important in determining the origin of switchbacks, as it is not yet clear whether each switchback is an isolated object, or if a patch of switchbacks are the sampling of a larger physical structure.

Horbury et al. (2020) provided the first piece of evidence of the 3D spatial structure of these switchbacks, using a perihelion stream to determine their structure as long and thin, with a high aspect ratio in roughly the radial direction. In this paper, we extend this idea to multiple solar wind streams. For the first encounter, PSP was connected to a small over-expanded coronal hole from the 29 October 2018 to the 13 November 2018, where the spacecraft then crossed the heliospheric current sheet and connected to a larger coronal hole between 14 November 2018 and 23 November 2018 (Badman et al. 2020). We have split the first encounter into 10 distinct solar wind streams, based on these patches and other enhancements in density and velocity. These streams are shown in Fig. 1, and will be referenced by the identification numbers shown above.

Global context for the second encounter with respect to the Sun's structure was inferred using white light images, which revealed that PSP sampled higher density solar wind when above the streamer belt (Rouillard et al. 2020). Therefore, the streams for encounter 2, as shown in Fig. 1, are based on this classification. The presence of switchbacks in both encounters therefore demonstrated that they exist in both slow and fast coronal hole streams as well as within and outside streamer belt flows.

We demonstrate that an average alignment direction can be found for switchbacks within each solar wind stream. We then compare the alignment direction for each stream to relevant physical directions, including the background flow and local Parker spiral (Parker 1958). Section 2 presents a theoretical discussion of how different physical properties combine to give a range of angles that the spacecraft can cut through the structure. This is followed by a discussion of how the average alignment direction was determined. Finally, the results are presented in Sect. 3, and their implications are discussed.

2. Method

In order to build up a 3D shape of a structure, it would be preferable to obtain multiple images from known angles to the structure in question. This technique has been applied to images of coronal mass ejections (De Koning et al. 2009; Liewer et al. 2009), but cannot be employed in the study of switchbacks due to their largely incompressible nature, meaning they would not be visible in images. Therefore, we are limited to single point spacecraft measurements, such as those provided by PSP during its first two encounters. An average shape can still be investigated from such observations, by studying how the apparent duration in the time series, t, varies with the direction at which

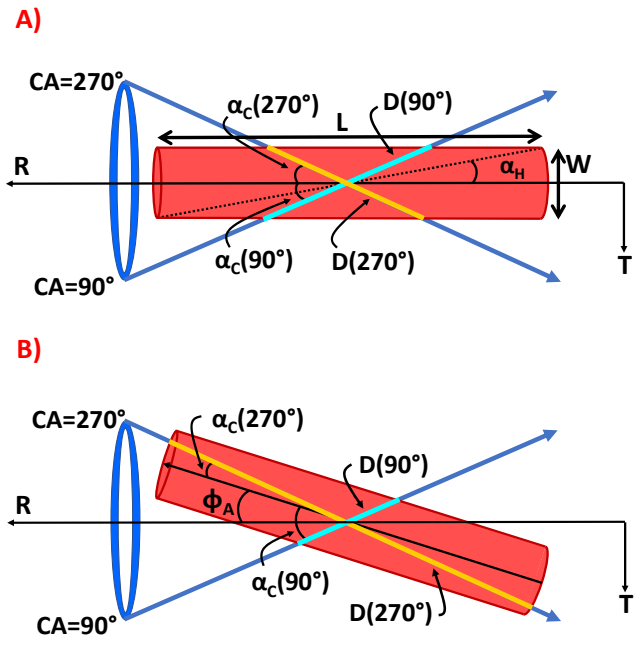

Fig. 2. (*a*) Example of two spacecraft cuts at a Clock Angle (CA) of 90° and 270° when viewed from the N direction. The ellipse represents the ring of possible velocities of the spacecraft from Fig. 3. In this example, the switchback structure (red cylinder) is centred on the ring of velocities, so both spacecraft cuts are at the same angle, and therefore only one value of D is measured. (*b*) In this example, the alignment direction of the switchbacks has been rotated by ϕ_A in the RT plane. This means that the spacecraft measures different values of D depending on the CA.

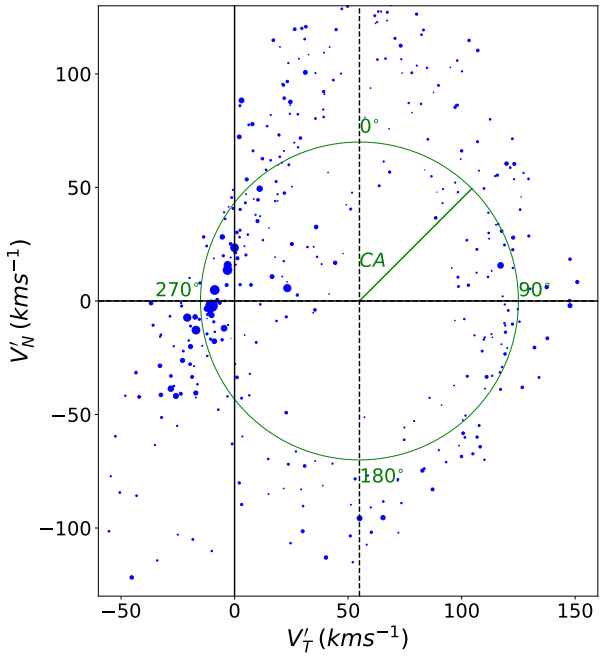

Fig. 3. T and N components of $V'_{\rm rel}$ for all the switchbacks in the E2S4 stream when rotated to coordinate system along $\hat{\boldsymbol{A}} = (-15°\phi_A, 0°\theta_A)$. They approximately lie on a circle (green) when projected into the TN plane, limiting the direction through which the spacecraft can cut the structures. The area of the points is proportional to the switchback duration, highlighting that this is a function of clock angle (CA).

the spacecraft cuts through the structure. For example, a 2D circle will have the same measured duration when cut through its centre, no matter which direction it is cut from, but an ellipse will have a larger measured duration when cut along its major axis. Inevitably, there will be a range of measured durations from the same cutting angle, as the structure can be sampled off centre, and the structures will not be perfectly uniform in size. Such considerations mean that analysis of their shape must be statistical in nature.

We assume a cylindrically symmetric long, thin structure, as suggested by Horbury et al. (2020), aligned along an alignment direction, $\hat{\boldsymbol{A}}$. The structure has width W and length, L, that can be seen in Fig. 2. The angle of the hypotenuse, $\alpha_{\rm H}$, is then defined as $\arctan\frac{W}{L}$, and gives a measure of the aspect ratio. The distance measured, D, by the spacecraft cutting through the centre at an angle, $\alpha_{\rm C}$ (cutting angle), is given by:

$$D = t \times |\boldsymbol{V}_{\rm rel}| = \begin{cases} \frac{W}{\sin\alpha_{\rm C}}, & \alpha_{\rm C} \geq \alpha_{\rm H} \\ \frac{W}{\tan\alpha_{\rm H}\cos\alpha_{\rm C}}, & \alpha_{\rm C} < \alpha_{\rm H}. \end{cases} \quad (1)$$

This analysis requires knowledge of the direction at which the spacecraft passed through each switchback. This can be estimated by first defining the velocity of the plasma relative to the spacecraft:

$$\boldsymbol{V}_{\rm rel} = \left\langle \boldsymbol{V}_{\rm pl} \right\rangle - \boldsymbol{V}_{\rm sc}, \quad (2)$$

where $\left\langle \boldsymbol{V}_{\rm pl} \right\rangle$ is the mean plasma velocity within the switchback relative to the Sun, using proton moments from the Solar Probe Cup (Kasper et al. 2016; Case et al. 2020). We use magnetic field measurements from the FIELDS instrument suite (Bale et al. 2016). The spacecraft velocity in Heliocentric Inertial frame, $\boldsymbol{V}_{\rm sc}$, has a large +T component at PSP's perihelion in the Radial–Tangential–Normal (RTN) coordinate system. In these coordinates, R points from the Sun to the spacecraft, N is the component of the solar north direction perpendicular to R, and T completes the right handed set. The cutting angle, $\alpha_{\rm C}$, is defined as the angle between $\boldsymbol{V}_{\rm rel}$ and $\hat{\boldsymbol{A}}$.

Ideally, the spacecraft would cut through the structure at many angles to build up a 3D shape. However, switchbacks are Alfvénic, meaning that magnetic and velocity perturbations are (anti-) correlated for (positive) negative polarity. Since Alfvénic fluctuations in the magnetic field lie on a sphere of constant radius, this corresponds to a sphere in velocity space, centred on some background velocity vector, with radius equal to the Alfvén speed (Bruno et al. 2004; Matteini et al. 2014, 2015). Switchbacks are deflections away from the background direction, and they rarely reach 180° (Woolley et al. 2020). Therefore, the possible values of $\left\langle \boldsymbol{V}_{\rm pl} \right\rangle$ create a torus in velocity space, which appears as a ring when projected in the TN plane, as demonstrated by Fig. 3. This then severely limits the possible angles that the spacecraft can sample the structure. The position of this ring is determined by the background velocity and the spacecraft velocity with the size being determined by the Alfvén speed, which in turn is affected by the local magnetic field strength and density.

In order to determine the effect of changing $\hat{\boldsymbol{A}}$, we first consider a scenario where the ring of velocity is centred on $\hat{\boldsymbol{A}}$, as shown in Fig. 2a. The ring of cutting angles can then be decomposed into the components $V'_{\rm rel,\,T}$ and $V'_{\rm rel,\,N}$, where $'$ denotes a coordinate system rotated so $\hat{\boldsymbol{A}}$ is along R, as done in Fig. 3. $V'_{\rm rel,\,T}$ and $V'_{\rm rel,\,N}$ follow a sine and cosine, respectively, as a function of CA. This is the clock face angle of the TN plane rotated

to the Parker spiral, so 0°, 90°, 180°, 270° correspond to +N, +T, −N, −T directions respectively.

Using these components α_C is given by:

$$\sin\alpha_C = \frac{\sqrt{V'^2_{\mathrm{rel,\,T}} + V'^2_{\mathrm{rel,\,N}}}}{|\boldsymbol{V}_{\mathrm{rel}}|}. \quad (3)$$

In this first example, α_C is constant for all clock angles, and therefore only one value of D is measured. This can be seen explicitly as these components follow a sine and cosine, meaning that the numerator of Eq. (3) is constant.

Figure 2b shows the structure rotated by ϕ_A in the RT plane. This introduces an offset in the $V'_{\mathrm{rel,T}}$ sine curve. This creates an asymmetry in α_C with CA when propagated through Eq. (3). This asymmetry is then reflected in D, which produces a range of durations seen in the time series data. In other words, the numerator of Eq. (3) is now a function of CA.

The aim of this study is to find the alignment direction that was most consistent with long, thin structures, where the alignment direction is defined by the angle in the RT plane, ϕ_A, and TN plane, θ_A. This concept is more explicitly stated as the combination of D and α_C that best followed Eq. (1). The length of the structure along the spacecraft trajectory, D, and $\boldsymbol{V}_{\mathrm{rel}}$ are observed quantities and do not depend on $\hat{\boldsymbol{A}}$. However, this is not true for the cutting angle, α_C, which is the angle between $\boldsymbol{V}_{\mathrm{rel}}$ and $\hat{\boldsymbol{A}}$. Therefore, each alignment direction we tested created a new set of α_C, while D remained the same.

We identified switchbacks as structures where the magnetic field deflected more than 45° away from the Parker spiral direction. We recognise that the start and end of the switchback is not when the structure deflects above this threshold. Therefore, we measured the duration of the identified switchback structure from when the deflection was above 30°, to best capture the full duration of the structures. The Parker spiral direction was calculated using twelve hour modes of the solar wind parameters, in an attempt to remove the switchback contribution (Bale et al. 2019). Successive switchbacks were merged if they were separated by less than 2 s.

In order to determine whether with the combination of α_C and D followed Eq. (1), we first binned the switchback data for a given stream into 2° bins in α_C. A minimum number of 10 points per bin was enforced in an attempt to remove statistically insignificant bins. Equation (1) only applies to cuts made through the centre of the structure. Therefore, we reduced the dataset to those switchbacks that are most likely to be cuts through the centre, by finding the maximum value of D for each bin. This removed situations where the spacecraft clipped the edge of the structure or encountered substructure that was not relevant to the average switchback shape.

This procedure allowed Eq. (1) to be fitted to D as a function of α_C for a stream, where the free parameters are W and α_H. A least squares algorithm was used, with constraints that $W > 0$ km and $0° < \alpha_H < 90°$ and a minimum of five bins in α_C were used. Functionally, α_H means that the longest switchbacks do not have to lie at 0° α_C and also provided an estimate of aspect ratio. The R^2 value of the fit was used to quantify the goodness of fit of the data to Eq. (1). This in turn allows for a determination of how consistent a particular alignment direction is with the underlying switchback direction for that stream. For each stream, the values of W and α_H were selected so that the value of R^2 was maximised. Of the sixteen streams outlined in Fig. 1, six streams produced robust results that are discussed in the next section.

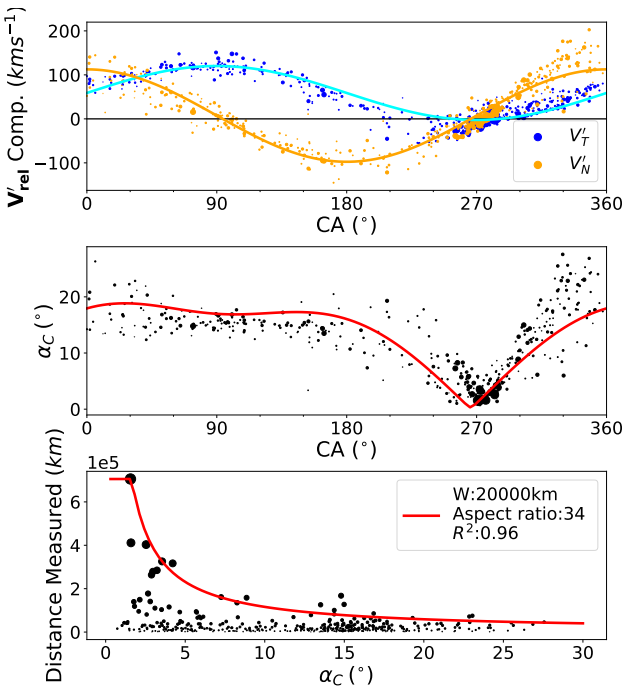

Fig. 4. Switchbacks for the E2S4 stream are shown to be consistent with long, thin structures along $\hat{\boldsymbol{A}} = (-15°\phi_A, 0°\theta_A)$. The fitting procedure in Sect. 2 gave values of $W = 20\,000$ km and a minimum aspect ratio of 34. The area of the scatter points are proportional to the distance measured by the spacecraft.

3. Results and discussion

The results for the E2S4 stream are shown in Fig. 4, with a best fit alignment direction of ($\phi_A = -15°, \theta_A = 0°$) that was found using the method outlined in Sect. 2. The top panel shows the $V'_{\mathrm{rel,\,T}}$ and $V'_{\mathrm{rel,\,N}}$ components, which follow a sine and cosine function as a function of CA that are offset from 0 km s^{-1}. This is simply unwrapping the ring presented in Fig. 3, with respect to the origin ($V'_{\mathrm{rel,\,T}} = 0$ km s^{-1}, $V'_{\mathrm{rel,\,N}} = 0$ km s^{-1}). The relationship between α_C and CA (middle panel) was calculated using Eq. (3), which produces a correlation between lower α_C and longer D. This is more explicitly demonstrated in the bottom panel where D is plotted as a function of α_C, with a best fit (red line) having a width of 20 000 km and a minimum aspect ratio of 34.

The width is a robustly determined quantity, with W in different streams varying from 20 000 km to 94 000 km with a mean of 56 000 km. We note that W appears to increase as the spacecraft moves further from the Sun (Fig. 5), although there is not a large enough spread in distance from the Sun to determine the rate of expansion. The aspect ratio ranges from 11 to 59 with a mean value of 28, although this parameter is only a lower bound, so should only be considered as being of the order of 10. Using these two average parameters the length of the structures, L, is ~500 000 km which is of the order of a solar radius.

The result of fitting Eq. (1) to stream E2S4 produced an R^2 of 0.96. The dependence of R^2 (only values greater than 0.8 are shown) with alignment direction can be seen in Fig. 5 for several solar wind streams. Each stream displays a tight grouping in R^2, indicating that there was a unique alignment direction. This grouping always has a negative ϕ_A, close to the local Parker spiral direction (red shading) which was also typically larger in amplitude than θ_A. In contrast, there was no correlation between switchback alignment direction and the background solar wind

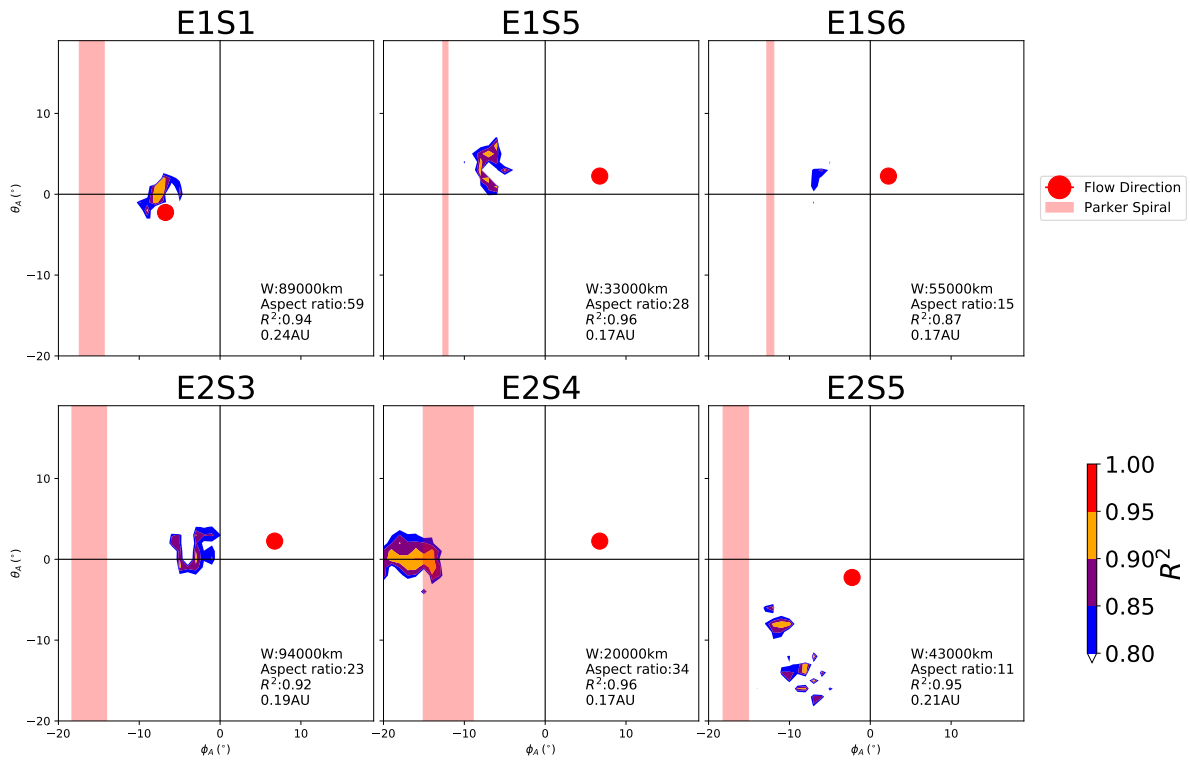

Fig. 5. Results of varying alignment direction, defined by the angle in the RT plane, ϕ_A, and TN plane, θ_A. The radial direction is the centre of the black cross hairs, with the Parker spiral and background flow direction also shown. The background flow direction is taken as the deHoffman–Teller frame (see Horbury et al. 2020), rather than the average velocity per stream which is influenced by the switchbacks. Higher scores correspond to an alignment direction most consistent with long, thin structures. This is always offset in -T direction, roughly consistent with Parker spiral direction calculated using a twelve hour mode of velocity.

flow direction (red dot). This suggests that the average switchback alignment direction is not related to the +T solar wind flow reported by Kasper et al. (2019). This statement does not rule out switchbacks as significant contributors to solar wind flow deflections, only that their longest axis is not aligned along the flow deflection.

However, this analysis does raise a subtlety when trying to interpret how switchbacks may be related to the background flow of the solar wind. The direction of magnetic deflection (which we discuss as clock angle) within each switchback affects the way in which the spacecraft cuts through it, since magnetic and velocity fluctuations are correlated. Therefore, the direction of magnetic deflection determines the apparent duration seen by the spacecraft, meaning that duration alone cannot be used as a proxy for the true physical size of a switchback. In other words, it would be false to argue that if an individual switchback has a longer duration at a spacecraft, it must be physically larger and therefore make a more significant contribution to the solar wind than one which is shorter. A more accurate approach would be to consider some metric that does not depend on duration, such as magnetic curvature or the Poynting flux (Mozer et al. 2020; Woolley et al. 2020). Both authors showed that the radial Poynting flux depends on the angle of magnetic deflection rather than duration, with a maximum reached at 90° from radial.

This relationship between deflection direction and apparent duration also means that the spacecraft data will include a sampling bias in the direction of the longest switchbacks' deflection. A simple average of all data within a stream will include a greater contribution from longer switchbacks. A consequence of this is that the average velocity direction will point along the deflection direction of the longest switchbacks, meaning that care must be taken when considering the average properties of a solar wind stream.

The analysis in Sect. 2 does not work for every stream, where either a pattern in duration could not be identified or there were not enough points to draw a solid conclusion. We note that this method may only apply in PSP's first three encounters, as these are times when the spacecraft was approximately co-rotating with the Sun's surface. As a result, plasma from the same source region was sampled for several hours (Bale et al. 2019), which allowed a large number of switchbacks to be observed per stream. Although PSP will pass through two co-rotation points per orbit, this window of co-rotation will become smaller with each orbit, reducing the number of switchbacks measured from the same source region. This would mean that the analysis in this paper may not be possible for PSP in future orbits, or indeed for other spacecraft at 1 AU.

We can nevertheless make an estimate of how switchbacks should appear in different situations in the heliosphere. Here we assume a constant aspect ratio, since we could not accurately determine how this varied with radial distance. For PSP's future orbits, if switchbacks are Parker spiral aligned then they will become more radial as distance to the Sun decreases, while the width would decrease. This, coupled with the greater spacecraft transverse velocity, means that the spacecraft will sample the structure at greater angles to their longest direction. Combined with their high aspect ratio, this means that the distribution of switchback duration will be more skewed towards shorter durations.

For larger radial distances from the Sun, the switchback alignment will be further from the radial direction. This, along with a lower spacecraft transverse velocity, will again lead to

the spacecraft travelling through the structure at larger angles. This should lead to longer duration switchbacks becoming more rare, although the rate at which switchback width increases could offset this. This was the case for Helios measurements where most velocity enhancements appeared as a single data point in measurements with a cadence of 40.5 s (Horbury et al. 2018). These are broad predictions as the true answer relies on a complex interplay between spacecraft speed; Alfvén speed; Parker spiral direction; background flow deflection; and the evolution of the switchbacks with distance.

4. Conclusion

We have investigated how the direction at which the spacecraft cuts through switchbacks influences the apparent duration that is seen in the time series data. We assumed that switchbacks are long, thin structures with cylindrical symmetry that are aligned in a certain direction, as suggested by Horbury et al. (2020). We then searched for the average alignment direction of switchbacks within several solar wind streams at ∼35−50 solar radii, and compared this to known physical directions. We found that this alignment direction was always away from radial, by ∼10°, with the same sense as the Parker spiral field. Although our assumptions cannot be proven with single spacecraft measurements, they produced consistent results repeated over six solar wind streams identified across the first two PSP encounters. The average width of the switchbacks, assuming cylindrical symmetry, was of the order of 50 000 km, with this width increasing as the spacecraft moved further from Sun. The aspect ratio of these structures was of order 10.

Our results show that each solar wind stream has its own average alignment direction, although this was similar across streams. Since PSP was co-rotating near perihelion, this may imply that differences in alignment direction between streams relates to the magnetic orientation of the source region – but this could also be due to switchbacks being instead guided by the local interplanetary magnetic field. If switchbacks are related to coronal jets, like those simulated by Roberts et al. (2018), it is more likely that an Alfvén wave packet launched by the jet would survive out to PSP, rather than the jet itself as discussed in Sterling & Moore (2020). The authors suggest that the length of such a wave-packet would be ∼600 000 km, similar to that from our results. It may be that a patch of switchbacks are the result of the spacecraft travelling inside a flux tube with coronal transients released intermittently at the base, with the quiet radial solar wind between these patches being the ambient solar wind predicted by Parker (1958). Our results do not rule out other possibilities for switchback origin however, such as the evolution of Alfvénic fluctuations (Squire et al. 2020).

We also remark that dips in the field magnitude associated with sharp magnetic deflections at the edge of switchbacks (Krasnoselskikh et al. 2020; Agapitov et al. 2020), along with their arc-polarised behaviour, are reminiscent of phase steepened Alfvén waves studied by Tsurutani and others (Tsurutani et al. 1994, 2002, 2005; Vasquez & Hollweg 1996). While it is not true of all switchbacks, there was a subset that demonstrated a slow rotation in the magnetic field followed by a sharp change back to the original field direction, and vice versa. A preliminary survey showed consistency of deflection direction for those switchbacks that exhibit sharp boundaries. This may suggest that these cases are linked to how the spacecraft cuts through the structure, with the sharp discontinuities being a part of the switchback structure, rather than a sampling effect. We intend to revisit this subject in a future study.

This analysis raises the point that the switchback duration in time series data is partly a consequence of spacecraft motion with respect to the switchback structures, rather than just a reflection of their true physical size. This means that it would be wrong to argue that larger duration switchbacks make a more significant contribution to the solar wind than those that are shorter. Indeed, it may be that those considered here, from PSP's first two perihelia while the spacecraft was near co-rotation, have longer durations at the spacecraft than those measured during later orbits when the spacecraft is moving considerably faster.

Acknowledgements. RL was supported by an Imperial College President's Scholarship, TSH by STFC ST/S000364/1, TW by ST/N504336/1, LDW by ST/S000364/1. SDB acknowledges the support of the Leverhulme Trust Visiting Professor program. S.T.B. was supported by NASA Headquarters under the NASA Earth and Space Science Fellowship Program Grant 80NSSC18K1201. The SWEAP and FIELDS teams acknowledge support from NASA contract NNN06AA01C. This work has made use of the open source and free community-developed space physics packages HelioPy (Stansby et al. 2020) and SpiceyPy (Annex et al. 2020). Parker Solar Probe was designed, built, and is now operated by the Johns Hopkins Applied Physics Laboratory as part of NASA's Living with a Star (LWS) program (contract NNN06AA01C). Support from the LWS management and technical team has played a critical role in the success of the Parker Solar Probe mission.

References

Agapitov, O. V., Dudok de Wit, T., Mozer, F. S., et al. 2020, ApJ, 891, L20
Annex, A., Pearson, B., Seignovert, B., et al. 2020, AndrewAnnex/SpiceyPy: SpiceyPy 3.1.1
Badman, S. T., Bale, S. D., Martínez Oliveros, J. C., et al. 2020, ApJ, 246, 23
Bale, S. D., Goetz, K., Harvey, P. R., et al. 2016, Space Sci. Rev., 204, 49
Bale, S. D., Badman, S. T., Bonnell, J. W., et al. 2019, Nature, 576, 237
Balogh, A., Forsyth, R. J., Lucek, E. A., Horbury, T. S., & Smith, E. J. 1999, Geophys. Res. Lett., 26, 631
Bowen, T. A., Bale, S. D., Bonnell, J. W., et al. 2020, ApJ, 899, 74
Bruno, R., Carbone, V., Primavera, L., et al. 2004, Ann. Geophys., 22, 3751
Case, A. W., Kasper, J. C., Stevens, M. L., et al. 2020, ApJS, 246, 43
De Koning, C. A., Pizzo, V. J., & Biesecker, D. A. 2009, Sol. Phys., 256, 167
Dudok de Wit, T., Krasnoselskikh, V. V., Bale, S. D., et al. 2020, ApJs, 246, 39
Horbury, T. S., Matteini, L., & Stansby, D. 2018, MNRAS, 478, 1980
Horbury, T. S., Woolley, T., Laker, R., et al. 2020, ApJS, 246, 45
Kasper, J. C., Abiad, R., Austin, G., et al. 2016, Space Sci. Rev., 204, 131
Kasper, J. C., Bale, S. D., Belcher, J. W., et al. 2019, Nature, 576, 228
Krasnoselskikh, V., Larosa, A., Agapitov, O., et al. 2020, ApJ, 893, 93
Liewer, P. C., De Jong, E. M., Hall, J. R., et al. 2009, Sol. Phys., 256, 57
Matteini, L., Horbury, T. S., Neugebauer, M., & Goldstein, B. E. 2014, Geophys. Res. Lett., 41, 259
Matteini, L., Horbury, T. S., Pantellini, F., Velli, M., & Schwartz, S. J. 2015, ApJ, 802, 11
Mcmanus, M. D., Bowen, T. A., Mallet, A., et al. 2020, ApJS, 246, 67
Mozer, F. S., Agapitov, O. V., Bale, S. D., et al. 2020, ApJS, 246, 68
Neugebauer, M., & Goldstein, B. E. 2013, in AIP Conf. Proc., 1539, 46
Parker, E. N. 1958, ApJ, 128, 664
Raouafi, N. E., Patsourakos, S., Pariat, E., et al. 2016, Space Sci. Rev., 201, 1
Roberts, M. A., Uritsky, V. M., DeVore, C. R., & Karpen, J. T. 2018, ApJ, 866, 14
Rouillard, A. P., Kouloumvakos, A., Vourlidas, A., et al. 2020, ApJS, 246, 37
Squire, J., Chandran, B. D. G., & Meyrand, R. 2020, ApJ, 891, L2
Stansby, D., Rai, Y., Argall, M., et al. 2020, heliopython/heliopy: HelioPy 0.13.0
Sterling, A. C., & Moore, R. L. 2020, ApJ, 896, L18
Szabo, A., Larson, D., Whittlesey, P., et al. 2020, ApJS, 246, 47
Tenerani, A., Velli, M., Matteini, L., et al. 2020, ApJS, 246, 32
Tsurutani, B. T., Ho, C. M., Smith, E. J., et al. 1994, Geophys. Res. Lett., 21, 2267
Tsurutani, B. T., Dasgupta, B., Galvan, C., et al. 2002, Geophys. Res. Lett., 29, 86
Tsurutani, B. T., Lakhina, G. S., Pickett, J. S., et al. 2005, Nonlinear Processes Geophys., 12, 321
Vasquez, B. J., & Hollweg, J. V. 1996, J. Geophys. Res.: Space Phys., 101, 13527
Verniero, J. L., Larson, D. E., Livi, R., et al. 2020, ApJS, 248, 5
Woodham, L. D., Horbury, T. S., Matteini, L., et al. 2021, A&A, 650, L1 (PSP SI)
Woolley, T., Matteini, L., Horbury, T. S., et al. 2020, MNRAS, 498, 5524

Appendix A: Stream summary

Table A.1. Summarising information for the streams used in this study including dates and number of switchbacks, with the results only shown for those streams where the analysis in Sect. 2 was successful.

ID	Start	End	Number	Source	R (AU)	ϕ_A (°)	θ_A (°)	R^2	W (km)	Aspect ratio
E1S1	31/10/2018 01:20	01/11/2018 10:53	239	CH	0.24	–8	0	0.94	89 000	59
E1S2	01/11/2018 16:56	02/11/2018 11:28	114	CH	0.22	–	–	–	–	–
E1S3	02/11/2018 11:35	03/11/2018 19:37	245	CH	0.2	–	–	–	–	–
E1S4	03/11/2018 20:13	04/11/2018 18:35	283	CH	0.18	–	–	–	–	–
E1S5	05/11/2018 00:48	05/11/2018 20:30	223	CH	0.17	–7	2	0.96	33 000	28
E1S6	05/11/2018 22:28	07/11/2018 09:30	510	CH	0.17	–6	3	0.87	55 000	15
E1S7	07/11/2018 09:54	08/11/2018 08:00	375	CH	0.18	–	–	–	–	–
E1S8	08/11/2018 17:50	09/11/2018 06:19	178	CH	0.19	–	–	–	–	–
E1S9	09/11/2018 14:23	10/11/2018 12:30	330	CH	0.21	–	–	–	–	–
E1S10	15/11/2018 17:23	19/11/2018 10:39	1054	CH	0.38	–	–	–	–	–
E2S1	30/03/2019 00:52	30/03/2019 18:36	214	NA	0.25	–	–	–	–	–
E2S2	30/03/2019 21:24	01/04/2019 08:30	295	NA	0.22	–	–	–	–	–
E2S3	01/04/2019 09:30	03/04/2019 08:00	285	Inside	0.19	–3	0	0.92	94 000	23
E2S4	03/04/2019 08:52	06/04/2019 11:49	435	Outside	0.17	–15	0	0.96	20 000	34
E2S5	06/04/2019 22:00	07/04/2019 18:19	198	Outside	0.19	–	–	–	–	–
E2S6	08/04/2019 03:50	09/04/2019 19:09	396	Inside	0.21	–7	–15	0.95	43 000	11

Notes. A graphical representation of these streams can be seen in Fig. 1. The radial distance (R) is the mean distance from the Sun within each stream. The source region is shown, with CH standing for coronal hole and Inside and Outside refer to the streamer belt.